Clays and Clay Minerals, Vol. 61, No. 2, 83–97, 2013.

STRUCTURAL CHARACTERIZATION OF REDUCED-CHARGE MONTMORILLONITES. EVIDENCE BASED ON FTIR SPECTROSCOPY, THERMAL BEHAVIOR, AND LAYER-CHARGE SYSTEMATICS

EVANGELOS N. SKOUBRIS[1], GEORGIOS D. CHRYSSIKOS[2], GEORGE E. CHRISTIDIS[1,*], AND VASSILIS GIONIS[2]

[1] Technical University of Crete, Department of Mineral Resources Engineering, Chania, Greece 73100
[2] Theoretical and Physical Chemistry Institute, National Hellenic Research Foundation, 48 Vass. Constantinou Ave., Athens, Greece 11635

Abstract—In the present study, the gradual layer-charge reduction of two Li-saturated smectites, SAz-1 from Arizona, USA, and FEO-G from Troodos, Cyprus, with octahedral charge of 0.54 electrons per half unit cell (e/huc) and 0.39 e/huc, respectively, was monitored by X-ray diffraction of K-saturated, ethylene glycol-solvated samples, by thermogravimetry-differential thermogravimetry, and by mid- and near-Fourier transform infrared spectroscopy after heating at 80−300ºC. With increasing heating temperature, the layer charge and cation exchange capacity (CEC) of both smectites decreased gradually due to Li fixation. At temperatures >200ºC, ~25% residual CEC was observed, suggesting incomplete Li fixation due to kinetic constraints. Dehydration of the original Li-smectites occurred in two steps, one peaking at ~100ºC and another at 175−180ºC. The latter decreased upon progressive Li fixation and vanished from smectites treated above ~125ºC. Dehydroxylation occurred at 635−640ºC in both smectites and was not affected by Li fixation. The second derivative analysis of the infrared spectra showed that Li fixation was manifested in both smectites by the growth of two new sharp OH-stretching fundamentals at ~3640 and 3670 cm^{-1} and their overtones at ~7115 and 7170 cm^{-1}. The new bands constitute pairs of fixed energy and relative intensity which grow simultaneously at the expense of the broad OH-stretching and overtone features of the original smectites. Based on this result, Li fixation is suggested to be accompanied by the simultaneous formation of two distinct trioctahedral-like structural OH species, which is compatible with Li^+ occupying *trans*-octahedral vacancies in both smectites.

Key Words—Attenuated Total Reflectance Spectroscopy, Hofmann-Klemen Effect, Layer Charge, Li Fixation, Near Infrared Spectroscopy, Residual Cation Exchange Capacity, Smectite, *Trans*-vacant.

INTRODUCTION

Smectites are clay minerals with important physical and chemical properties, stemming from their crystal-chemical characteristics, their very small particle size, and the correspondingly large specific surface area. Properties of smectite valued by industry include CEC, swelling and rheological properties, hydration and dehydration, high plasticity, bonding capacity, and the ability to interact with inorganic and organic reagents (Odom, 1984). A key determinant of these properties is the layer charge which is due to substitutions in the tetrahedral and/or the octahedral sheet, or to the existence of vacancies in the octahedral sheet. The layer charge is associated with CEC and ion-exchange selectivity (Maes and Cremers, 1977, 1978; Shainberg *et al.*, 1987; Güven, 1992; Laird, 1999). Layer charge has been shown to be related also to the colloidal properties of smectites such as swelling (Slade *et al.*, 1991; Laird, 2006; Christidis *et al.*, 2006), especially if heterogeneity in charge magnitude and localization is also considered (Christidis and Eberl, 2003). Moreover, the magnitude of the layer charge is related to the adsorption of organic compounds on the smectite surface (Laird *et al.*, 1992).

Reduced-charge smectites result from the thermal treatment of Li-saturated dioctahedral smectites with octahedral charge. The process, known as the Hofmann-Klemen effect (Hofmann and Klemen, 1950), leads to the reduction of the layer charge and is manifested by the decrease in the CEC and the loss of the expandable character of the smectites. Apparently, heating induces the dehydration of Li cations and their migration into the layer structure of the mineral, where they become fixed, *i.e.* resistant to cation exchange. Suggested positions of Li^+ ions in the structure include the vacant octahedral sites (Hofmann and Klemen, 1950; Green-Kelly, 1953; Sposito *et al.*, 1983; Srasra *et al.*, 1994; Muller *et al.*, 1997; Stackhouse and Coveney, 2002; Madejová *et al.*, 2006), the ditrigonal cavities of the tetrahedral sheet (Tettenhorst, 1962; Luca *et al.*, 1989; Alvero *et al.*, 1994; Theng *et al.*, 1997), or both (Brindley and Ertem, 1971; Calvet and Prost, 1971; Madejová *et al.*, 1996; Karakassides *et al.*, 1999). The Hofmann-Klemen effect is specific to smectites with octahedral charge and was initially proposed as a method to distinguish montmorillonite from beidellite, a 2:1 phyllosilicate with tetrahedral layer charge (Green-Kelly, 1953).

* E-mail address of corresponding author:
christid@mred.tuc.gr
DOI: 10.1346/CCMN.2013.0610207

The aforementioned structural interpretations all stem from a remarkably uniform phenomenology of the Hofmann-Klemen effect. The amount of fixed Li^+ increases with temperature (Calvet and Prost, 1971) and reaches a plateau at ~220ºC (Brindley and Ertem, 1971; Komadel *et al.*, 1996). This result is common to many different smectites with variable composition and layer charge (Komadel *et al.*, 1996; Gates *et al.*, 2000; Madejová *et al.*, 2000a, 2000b; Bujdák *et al.*, 2001). In all these studies the reduction of layer charge with Li fixation was monitored indirectly by measuring the CEC of the smectites. Interestingly, Li^+-exchanged montmorillonite samples heated to complete fixation display CEC values that are greater than those expected from the complete reduction of their octahedral charge (Brindley and Ertem, 1971; Lim and Jackson, 1986; Jaynes and Bigham, 1987; Komadel, 2003). For example, a Li^+-exchanged Otay montmorillonite (SCa-2) with ~95% octahedral charge was reported to undergo a reduction of CEC by only 81% as a result of heating at 300ºC (Hrobáriková *et al.*, 2001; Komadel, 2003). The observed discrepancy has been attributed to the existence of mechanisms of Li fixation which do not lead to charge reduction (*e.g.* fixation in the interlayer and/or replacement of the structural OH groups by O^-Li^+, Jaynes and Bigham, 1987) or to the incomplete replacement of exchangeable cations during the initial Li-exchange process (Hrobáriková *et al.*, 2001).

Since the early work of Calvet and Prost (1971), infrared (IR) spectroscopy has been by far the most widely used technique for the structural characterization of reduced-charge smectites. Mid- and near-IR studies on Li-exchanged and heated (>120ºC) montmorillonite samples have linked the Hofmann-Klemen effect to the appearance of new sharp absorption bands corresponding to the stretching, bending, combination, and overtone modes of structural OH groups (Sposito *et al.*, 1983; Madejová *et al.*, 1996; 2000a, 2000b; Hrobáriková *et al.*, 2001; Gates, 2005; Madejová, 2005; Madejová and Komadel, 2005). By analogy to trioctahedral smectites which also exhibit sharp OH bands at similar positions (Russell and Fraser, 1994), the IR spectra of reduced-charge montmorillonites have been interpreted as suggesting the formation of local trioctahedral domains of the AlMgLiOH or AlAlLiOH types (Calvet and Prost, 1971; Srasra *et al.*, 1994; Madejová *et al.*, 2000a, 2000b). Alternatively, based on an earlier study on micas (Besson and Drits, 1997a, 1997b), Zviagina *et al.* (2004) assigned the new OH bands to pyrophyllite-like fragments in the dioctahedral 2:1 phyllosilicates.

The present study revisits the structural aspects of layer-charge reduction of two nearly ideal montmorillonites (*i.e.* with negligible tetrahedral charge) which differ in terms of octahedral charge. In addition to determining the CEC of the samples with progressively reduced charge, Li fixation was monitored by systematic measurements of the layer charge by X-ray diffraction (XRD) after K-saturation (Christidis and Eberl, 2003). In principle, the use of layer charge as a proxy to monitor Li fixation is more appropriate than CEC, as it records directly the outcome of the Hofmann-Klemen effect. The monitoring of Li fixation with layer-charge measurements was reported by Maes *et al.* (1979). However, the alkylammonium method employed by these latter authors has been suggested to underestimate layer charge by up to 40% (Laird and Fleming, 2008).

In addition to layer-charge measurements, the same samples were evaluated by attenuated total reflectance in the mid-IR (ATR-FTIR) range and diffuse reflectance (DRIFT) in the near-IR range. Besides allowing comparisons with previous literature, the aim of this vibrational investigation was to bring forward a more detailed study of the sharp features which develop upon fixation by taking advantage of second derivative analysis (Gionis *et al.*, 2006, 2007). Finally, the study is complemented by thermogravimetric analysis (TGA) to allow for the quantitative assessment of dehydration and dehydroxylation in reduced-charge montmorillonites as a function of heating temperature and to build on early results by Alba *et al.* (1998).

MATERIALS AND METHODS

Preparation of reduced-charge samples

Reduced-charge montmorillonite (RCM) preparations were based on two samples with minimum tetrahedral and different octahedral charge: SAz-1 (The Clay Minerals Society Source Clays Repository) is a typical high-charge montmorillonite and FEO-G (Christidis, 2006) is a low-charge montmorillonite from the Polycanthos area, Cyprus. Both samples have a small Fe content. Their chemical compositions (microprobe analysis, <0.2 μm fraction) and structural formulae are compared in Table 1. According to these analyses, the layer charge of neat SAz-1 and FEO-G are 0.54 and 0.39 e/huc, respectively (Gates, 2005; Christidis, 2006). The RCMs were prepared from the <2 μm fraction of SAz-1 and from a hand-crushed sample of FEO-G, due to the limited availability of the latter stock material. The SAz-1-based RCMs contain minor quartz and feldspar (2.5% in total) and clinoptilolite (1%) and the FEO-G-based RCMs contain minor quartz (4%), kaolinite (~3%), opal-CT, and illite (1−2%) (Christidis, 2006). The two clays were saturated with Li^+ at ambient temperature (for 2×12 h in 1 M LiCl solution, at a 1:100 clay/LiCl solution ratio), washed with ethanol until free of excess salts ($AgNO_3$ test), dried at 60ºC, and crushed with pestle and mortar. This standard experimental approach was assumed to lead to complete Li saturation (Bain and Smith, 1987). Portions (~500 mg) of these Li-saturated samples were heated for 24 h to a temperature in the range 60−300±5ºC. These samples are referred to as LiSAz-1_xxx or LiFEO-G_xxx, where xxx indicates the heating temperature. Due to sample shortage, Li-FEO-G was heated only at 60, 120, 200, and 300ºC.

https://doi.org/10.1346/CCMN.2013.0610207 Published online by Cambridge University Press

Table 1. Chemical analysis and structural formulae of the SAz-1 montmorillonite (Gates, 2005) and the FEO-G montmorillonite (Christidis, 2006). The chemical composition of FEO-G was obtained from microprobe analysis. The chemical analysis of SAz-1 was reported on a LOI-free basis.

	FEO-G	SAz-1
SiO_2	60.67	67.59
Al_2O_3	21.05	19.85
Fe_2O_3	0.87	1.71
MgO	3.81	6.508
CaO	0.5	3.919
Na_2O	2.24	0.118
TiO_2	N/A	0.28
MnO	N/A	0.035
K_2O	0	0.074
Total	89.13	100.08
Structural formulae based on $O_{10}(OH)_2$		
Tetrahedral cations		
Si	3.97	3.99
Al^{IV}	0.03	0.01
Octahedral cations		
Al^{VI}	1.60	1.38
Fe^{3+}	0.04	0.07
Mg	0.36	0.56
Interlayer cations		
Ca	0.04	0.25
Mg	0.01	
Na	0.29	0.03
K	0	0
Layer charge	0.39	0.54
Interlayer charge	0.39	0.53
Tetrahedral charge (%)	7.7	2

Determination of layer charge and CEC

Layer charge was determined according to the method described by Christidis and Eberl (2003). The original samples and RCM preparations were K-saturated with 1 M KCl solutions, washed free of excess salts ($AgNO_3$ test), transferred to glass slides to make oriented clay mounts, left to dry at ambient temperature, and finally exposed to ethylene-glycol vapor at 60ºC overnight. The ethylene glycol-solvated samples were examined by XRD (Bruker AXS D8 Advance diffractometer) in the range 2–35º2θ, using CuKα radiation, with a step size of 0.02º2θ and 0.3 s counting time per step. The layer charge was determined on the basis of the XRD data using the *LayerCharge* computer code (Christidis and Eberl, 2003). A conservative estimate of the error associated with this determination of the layer charge is ±0.02 e/huc. The method has a lower threshold for determination of layer charge of 0.39 e/huc, which precluded the study of FEO-G-based RCMs.

The CEC of all samples was determined with a homebuilt Kjeldahl microsteam apparatus, after saturation with 1 M ammonium acetate at pH 7. Approximately 300 mg of each sample was saturated twice overnight with 10 mL of 1 M ammonium acetate, washed free of excess salts, and heated together with excess NaOH (~30 mL, 5 N) in the Kjeldahl reactor. The product of the distillation (ammonia) was collected in a conical flask containing 25 mL of boric acid (1 N) and methyl red and bromocresol green indicators, followed by titration with 0.05 N sulfuric acid. The error associated with this titration is of the order of ±2 cmol/kg, but the error of the overall determination is larger for samples with very low CEC, due to difficulties associated with their expansion and NH_4^+ exchange. The CEC data are expressed per 100 g of clay dried at 260ºC, using the weight-loss results obtained from TGA (see below). Before CEC determination, the samples had been dried at 60ºC. Drying at 105ºC was avoided because Li migration was observed to take place at this temperature.

TGA and IR spectroscopy

Small portions of each sample (~50 mg) were analyzed with an automated TGA system (TGA-6, Perkin Elmer). Both TG and DTG curves were obtained. The samples were heated gradually from 40 to 900ºC at a heating rate of 10ºC/min under a flow of dry N_2 gas. The sample weight was measured at intervals of 1.5ºC. The dehydroxylation temperatures were obtained from the DTG curves.

All IR spectra were measured on neat powder samples equilibrated to ambient temperature (25ºC, 30–35% RH). Mid-IR spectra (525–4000 cm^{-1}) were measured on a Fourier-transform instrument (Equinox 55 by Bruker Optics) equipped with a single-reflection diamond ATR accessory (DuraSamplIR II by SensIR Technologies). Contact between the powder samples and the diamond element was ensured by a suitable press, applying a pressure of ~100 MPa. Each spectrum represents the average of 300 scans recorded at an optical resolution of 2 cm^{-1} (digital resolution 1 cm^{-1}). The spectra are shown in the absorption mode after correction for the wavelength dependence of the penetration depth. The NIR spectra (3600–12000 cm^{-1}) were measured on a Fourier-transform spectrometer (Vector 22/N by Bruker Optics) equipped with an integrating sphere accessory. All spectra were measured against a gold reference and shown in the absorption mode. Each spectrum is the average of 200 scans at an optical resolution of 4 cm^{-1} and digital resolution of 2 cm^{-1}. The 2nd derivatives of the mid- or near-IR absorption spectra were calculated using the Savitzky-Golay algorithm (*Opus* software, Bruker) to allow for the identification of weak sharp features overlapping with broad bands. Typically, a 13-point smoothing window was employed, unless otherwise indicated.

https://doi.org/10.1346/CCMN.2013.0610207 Published online by Cambridge University Press

RESULTS AND DISCUSSION

Layer charge and CEC of the reduced-charge smectites

Application of the Greene-Kelly test to SAz-1 at different temperatures resulted in systematic variations of the XRD traces of K-saturated, ethylene glycol-solvated samples (Figure 1). These XRD traces are comparable to those of natural samples and suggest a progressive change from high-charge to low-charge smectite. The first-order reflection peak of the K-saturated LiSAz-1_060 occurred at 6.42º2θ (d_{001} = 13.7 Å), and shifted gradually upon heating at 135ºC to 5.14º2θ (d_{001} = 17.1 Å). The XRD traces of samples LiSAz-1_060-100 exhibited d_{001} spacings of <15 Å and d_{003} spacings at ~4.70 Å. These traces are, therefore, typical of high-charge smectites (layer charge >0.475 e/huc) according to Christidis *et al.* (2006). RCMs heated between 105 and 115ºC exhibited d_{001} at 16.5−15.5 Å and irrational *d* spacings of higher-order basal reflections which are typical of smectites with intermediate layer charge (0.46−0.44 e/huc). Heating at 120−135ºC decreased the layer charge further, as in low layer-charge smectites (0.42−0.39 e/huc) which are characterized by a >16.6 Å 001 diffraction maximum and rational, higher-order basal reflections (Christidis *et al.*, 2006). Above 130ºC, the first-order reflection decreased quickly in intensity while remaining fixed in position (Figure 1). Indeed, the layer charge of

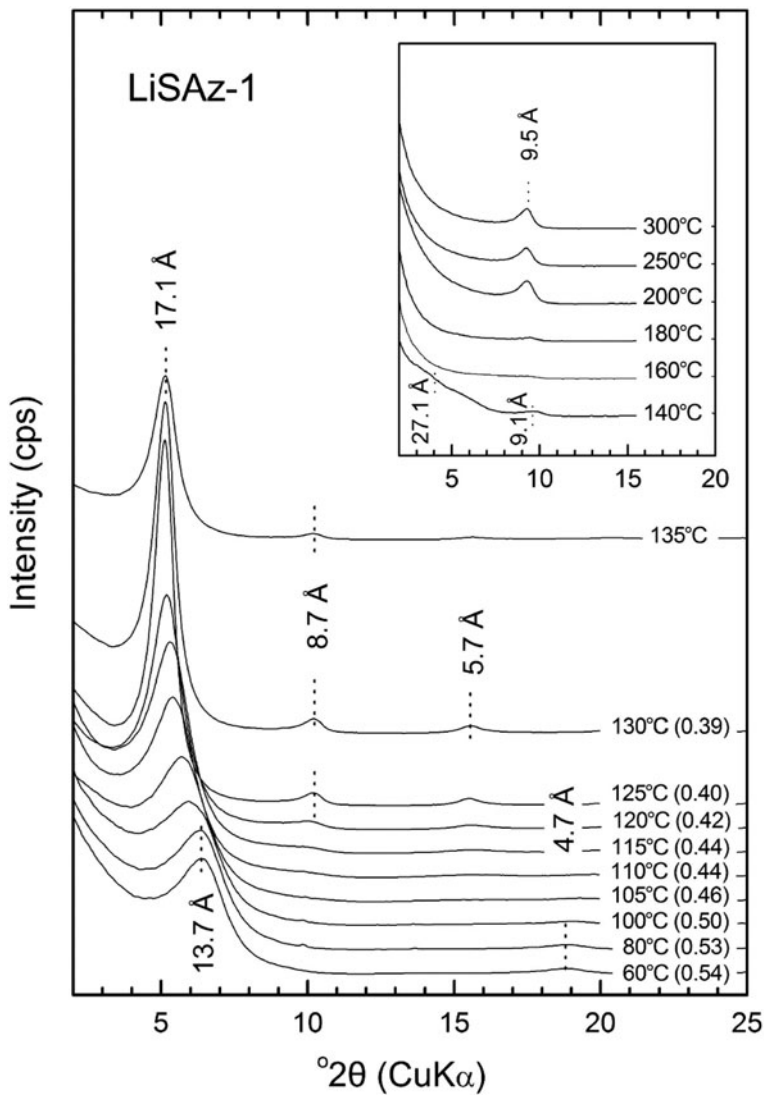

Figure 1. Room-temperature XRD patterns of K-saturated and ethylene glycol-solvated LiSAz-1 samples previously subjected to heating in the 60−135ºC range for 24 h. Note the shift of d_{001} from ~13.7 Å (60ºC) to 17.1 Å (135ºC). Charges (e/huc) calculated according to Christidis and Eberl (2003) are shown in parentheses. The inset shows the patterns of the corresponding samples heated at higher temperatures and up to 300ºC. Note the appearance of a new peak ~9.5 Å which is indicative of collapsed montmorillonite layers.

https://doi.org/10.1346/CCMN.2013.0610207 Published online by Cambridge University Press

LiSAz-1_130 and LiSAz-1_135 was found to be 0.39 e/huc (Table 2) and was probably overestimated because this value coincides with the detection limit of the Christidis and Eberl (2003) method. For the same reason, the layer charges of LiFEO-G-based RCMs cannot be estimated correctly. Samples LiSAz-1_140–180 displayed broad diffraction maxima between 4 and 5º2θ and another diffraction maximum at ~9.8º2θ (9.1 Å), indicating the existence of a superstructure due to ordered interstratification of totally collapsed and expandable smectite layers. The progressive appearance of a new diffraction maximum with d = 9.5 Å in samples LiSAz-1_180–300 indicated the presence of completely collapsed montmorillonite layers (Sato *et al.*, 1992). The lack of a diffraction maximum at 5º2θ in these samples was compatible with the negligible tetrahedral charge of SAz-1. This is because montmorillonites with a significant proportion of tetrahedral charge display diffraction maxima both at 5º2θ and at 9.3º2θ, after the completion of the Greene-Kelly test, due to the existence of discrete phases or to mixed-layer montmorillonite-beidellite (Lim and Jackson, 1986; Guisseau *et al.*, 2007). Application of the Greene-Kelly test to FEO-G at 120, 200, and 300ºC yielded identical results to SAz-1 (data not shown). In summary, the position of the 001 diffraction maximum was not affected after heating at 120ºC, but shifted to ~9.3º2θ (9.5 Å) after heating at 200 and 300ºC.

The CEC values of LiSAz-1 sample series (Table 2) displayed a sigmoidal dependence on the heating temperature from ~130 to ~40 cmol/kg with a midpoint at ~120ºC (Figure 2). The overall trend is similar to that reported by Madejová *et al.* (2000a, 2000b) and Bujdák *et al.* (2001), the main difference being the smaller final CEC value reported by the latter authors. Fewer data points exist for the LiFEO-G system, but the observed % reduction of the CEC with heating temperature was comparable to that of LiSAz-1, suggesting that the two montmorillonites respond to Li fixation in a very similar manner despite differences in their initial layer charge.

Measured layer charges follow well the trend of the CEC data up to 120–125ºC, and then level off toward 0.39 e/huc (Figure 2, inset). This value is the lower detection limit of the layer-charge determination method employed, because it corresponds to a material consisting solely of low-charge smectitic layers (Christidis and Eberl, 2003). Interestingly, a similar leveling off was observed in the data of Maes *et al.* (1979) who used the alkylammonium method to measure the layer charges of RCMs based on montmorillonite from Camp Berteau (Morocco).

The CEC of the Li samples heated at temperatures >200ºC was greater than that expected from complete charge reduction and the residual CEC did not depend on the layer charge of the original samples (Figure 2). The compensation of deprotonated hydroxyl groups (Jaynes and Bigham, 1987) and the incomplete replacement of exchangeable cations during Li-exchange (Hrobarikova *et al.*, 2001) might explain the observed trends. However, the former option, while significant in the case of Fe-rich smectites including nontronites (Russell, 1979; Jaynes and Bigham, 1987), is less important in the case of Al-Mg, Fe-poor montmorillonites, especially

Table 2. CEC, layer charge, weight % loss in the 40–260ºC, and dehydroxylation regions of the reduced-charge LiSAz-1 and LiFEO-G samples. Weight loss % data are expressed with reference to the weight of the samples at 260ºC.

Sample	CEC (cmol/kg)	% of CEC_{060}	Layer charge (e/huc)	Weight loss, % (40–260ºC)	Weight loss, % (260–900ºC)
LiSAz-1_060	131.6	100.00	0.54	16.45	4.58
LiSAz-1_080	131.6	100.00	0.53	16.45	4.58
LiSAz-1_100	126.7	96.25	0.50	15.87	4.53
LiSAz-1_105	119.9	91.12	0.46	15.29	4.48
LiSAz-1_110	113.8	86.49	0.44	15.26	4.58
LiSAz-1_115	107.7	81.86	0.44	14.61	4.50
LiSAz-1_120	96.1	73.05	0.42	12.21	4.78
LiSAz-1_125	89.8	68.21	0.40	9.81	5.07
LiSAz-1_130	75.6	57.42	0.39	9.15	5.18
LiSAz-1_135	62.2	47.29	(0.39)	6.94	5.77
LiSAz-1_140	57.7	43.84	–	5.41	5.27
LiSAz-1_160	53.2	40.39	–	3.88	4.92
LiSAz-1_180	46.5	35.37	–	3.01	5.23
LiSAz-1_200	34.8	26.45	–	2.33	5.70
LiSAz-1_250	36.7	27.89	–	1.95	4.83
LiSAz-1_300	39.5	30.04	–	2.11	5.03
LiFEO-G_060	89.2	100.00	0.39	9.09	5.89
LiFEO-G_120	67.7	75.93	–	5.92	5.78
LiFEO-G_200	29.0	32.52	–	2.33	5.37
LiFEO-G_300	24.3	27.25	–	2.15	5.05

https://doi.org/10.1346/CCMN.2013.0610207 Published online by Cambridge University Press

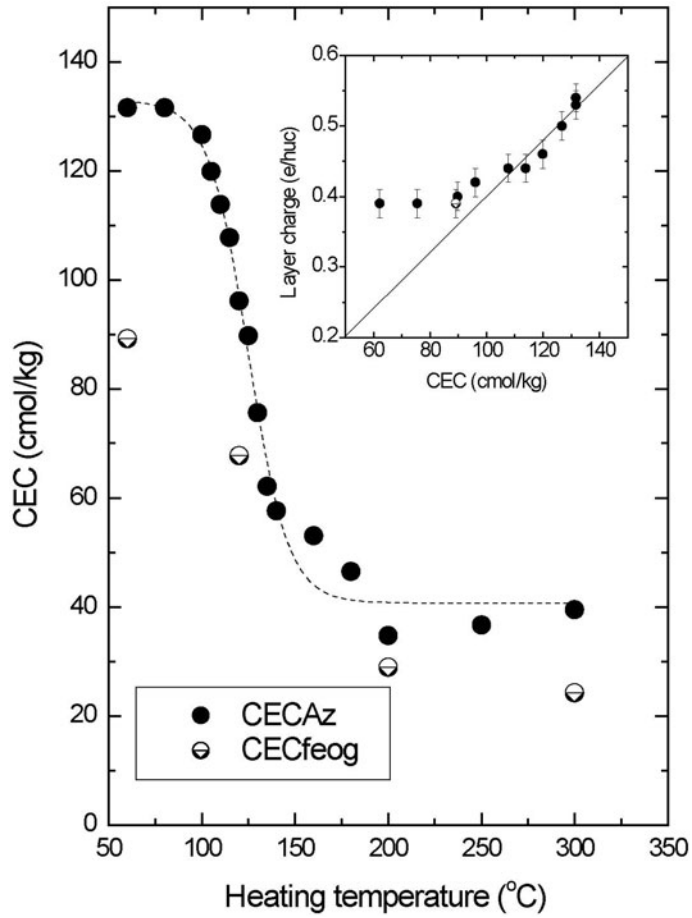

Figure 2. Dependence of CEC on the heating temperature of LiSAz-1 and LiFEO-G. The sigmoidal line is a guide to the eye through the LiSAz-1 dataset. The inset compares the layer charge and CEC data of the same samples (Table 2).

those with low layer charge (Jaynes and Bigham, 1987), such as the FEO-G examined here. Also, incomplete Li exchange is not considered significant because the two smectites studied displayed similar behavior, although they had different layer charge. Indeed, had this been the case, the fraction of the residual CEC would have been smaller in the low-charge FEO-G smectite (*e.g.* Maes and Cremers, 1978).

The possible influence of variable charge on the residual CEC was also examined. The CEC calculated from the structural formulae for the layer charges of the original and the RCMs (Table 1) was compared to the CEC from ammonium acetate. The difference between the two values varied from +7.1 to −7.7% with respect to the ammonium acetate CEC, the average difference being ~+1% of the CEC. The CEC of the original FeO-G determined by ammonium acetate is almost identical to the CEC derived from Table 1, assuming 5% structural H_2O, *i.e.* 99.1 cmol/kg (104.5 cmol/kg on an anhydrous basis). The <2 μm fraction of FeO-G contains ~8−9% impurities (3% kaolinite, 4% quartz, the rest being opal-CT and illite). The CEC of pure smectite determined by ammonium acetate was, therefore, 97−98 cmol/kg (102−103 cmol/kg on an anhydrous basis) *i.e.* almost identical to the value calculated. Similarly, the CEC of SAz-1 calculated from Table 1 was 136.1 cmol/kg (143.3 cmol/kg on an anhydrous basis). The sample contained ~2.5% quartz and feldspar and ~1% clinoptilolite. Clinoptilolite increased the CEC determined by ammonium acetate by ~0.6 cmol/kg. Hence the actual CEC of the SAz-1 smectite as determined by ammonium acetate is 134.4 cmol/kg (141.5 cmol/kg on an anhydrous basis). Therefore, the variable charges in the present case cannot explain the residual CEC. This is expected, as the CEC measurements were performed at pH 7, *i.e.* close to the iep of the edges of smectite (*e.g.* Tombacz and Szekeres, 2004).

An alternative explanation is to consider that the Green-Kelly test does not lead to complete reduction of the octahedral layer charge. By definition, smectites have layer charges of 0.2−0.6 e/huc and swell under addition of glycerol and/or ethylene glycol vapors (Brigatti *et al.*, 2006). Hence, 2:1 phyllosilicates with layer charges of <0.2 e/huc are not expected to swell.

https://doi.org/10.1346/CCMN.2013.0610207 Published online by Cambridge University Press

Interstratification between collapsed layers and swelling layers was observed in samples heated at 140ºC but was absent from samples heated at higher temperatures (Figure 1). Hence, in samples heated above 200ºC the possible remaining empty octahedral sites next to Mg-bearing octahedral sites are not clustered in swelling domains but are randomly dispersed. Such an arrangement of octahedra which were not occupied by Li for the SAz-1 montmorillonite (Figure 3) would not cause swelling of the smectite layers. Indeed, if 25% of the available octahedra remained vacant, they would account for residual layer charge of 0.145 e/huc or a CEC of 35 cmol/kg, observed in the present study.

TGA analysis

The DTGA thermograms of the RCMs based on LiSAz-1 exhibited a systematic dependence on the temperature of Li fixation (Figure 4). This dependence was mainly manifested by drastic changes of the low-temperature thermogravimetric envelope (<260ºC) in terms of both complexity and integrated intensity. Events in this range are attributed to dehydration processes. The first event, peaking at ~100ºC in LiSAz-1_060, corresponds to the loss of adsorbed water.

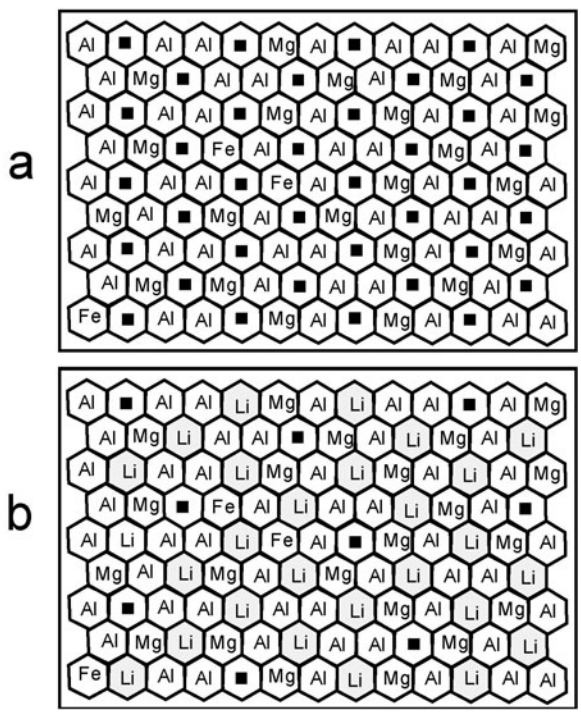

Figure 3. Schematic diagram showing the process of incomplete charge reduction in SAz-1 Li-montmorillonite heated at temperatures >200ºC. (a) Representation of the octahedral sheet of SAz-1 montmorillonite. (b) Representation of the octahedral sheet after charge reduction. 25% of the vacant octahedra were not filled by Li during the Green-Kelly test. The octahedra with black squares are vacant, whereas those shaded are filled with Li.

A second event, centered at 175−180ºC, was observed as a shoulder in samples subjected to low fixation temperatures. Its amplitude decreased abruptly at temperatures exceeding 115ºC and vanished at ~130ºC, *i.e.* a range which coincides with the appearance of interstratified structures between collapsed and swelling smectite layers (Figure 4). A similar high-temperature dehydration event has typically been observed in smectites saturated with Ca^{2+}, Mg^{2+}, or Li^{+} and attributed to H_2O in the coordination sphere of these high field strength interlayer cations (Alba *et al.*, 1998). An alternative explanation to H_2O interacting with localized tetrahedral charge (Koster van Groos and Guggenheim, 1987) should be ruled out in the case of SAz-1 and FEO-G.

The total weight % loss in the 40−260ºC range is expressed against the weight measured at 260ºC and is included in Table 2. This quantity exhibits a sigmoidal dependence on the fixation temperature which is similar to that of CEC (Figure 2) and, therefore, weight % loss and CEC are linearly related (R^2 = 0.97, σ = 1 wt.%, graph not shown). Finally, the high-temperature event in the DTGA data corresponds to the dehydroxylation of the smectite. It was observed (Figure 4) as nearly independent of the Li-fixation temperature in both position (635−640ºC) and integrated intensity (4.9±0.4 wt.%, Table 2). The dehydroxylation temperature of the RCMs based on LiSAz-1 is very similar to that of neat SAz-1 montmorillonite (633−639ºC, Guggenheim and Koster van Groos, 2001) and the corresponding weight % loss was identical to that predicted theoretically (4.8 wt.%). The four RCM samples based on LiFEO-G exhibited very similar phenomenology (Table 2). The greater weight loss observed was compatible with the presence of minor kaolinite.

IR spectroscopy

The ATR and NIR spectra of several RCMs based on LiSAZ-1 and spanning the whole range of fixation temperatures (60−300ºC) are shown in Figure 5. Besides trivial details due to differences in the optical setups employed, these spectra are identical to those published by Madejová *et al.* (2000a, 2000b) for the same system. In agreement with the TGA data, both spectral series are characterized by the very pronounced intensity reduction of H_2O bands upon increasing fixation temperature. These bands dominate the spectra at 1635 cm^{-1}, 3000−3900 cm^{-1}, 4900−5400 cm^{-1}, and 6500−7300 cm^{-1}, and correspond to the bending (δ), stretching (ν_{01}), combination ($\nu_{01}+\delta$), and 1st overtone stretching (ν_{02}) envelopes, respectively (Bishop *et al.*, 1994). Subtler but important changes were also observed in all other frequency ranges, including those of the structural OH-bending vibrations (950−675 cm^{-1}), Si−O stretching vibrations (1175−950 cm^{-1}), OH-stretching vibrations (3500−3700 cm^{-1}), combination modes (4300−4600 cm^{-1}), and overtone modes (7000−7200 cm^{-1}). Overall, Li fixation appeared to

https://doi.org/10.1346/CCMN.2013.0610207 Published online by Cambridge University Press

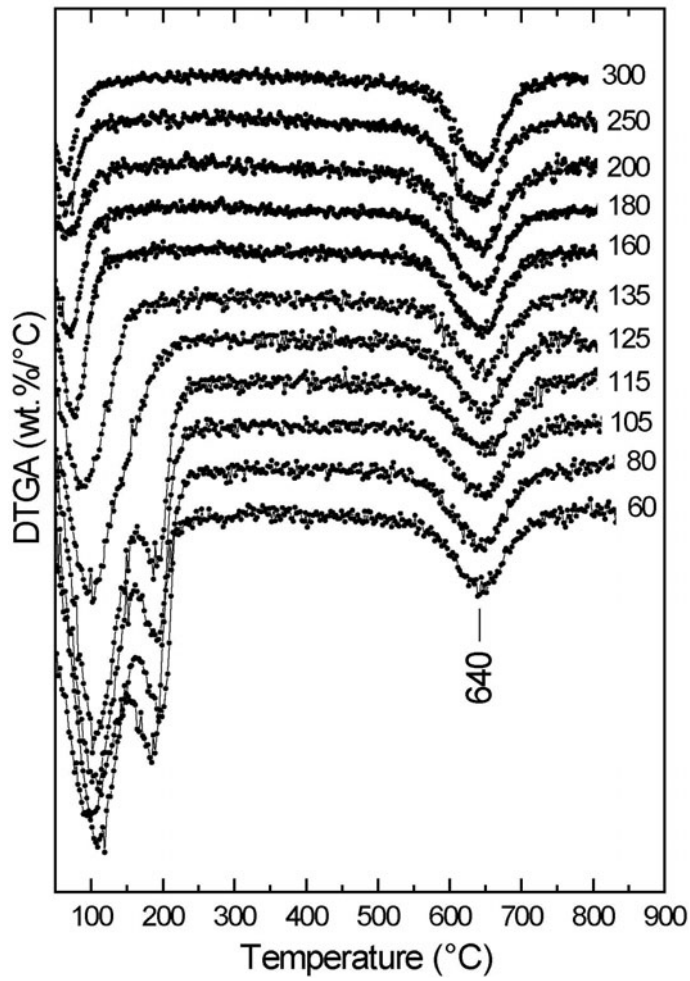

Figure 4. DTGA diagrams of the reduced-charge LiSAz-1 samples series as a function of heating in the 60−300ºC range. The data have been normalized to the weight of the samples at 260ºC and are shown offset for clarity.

involve the emergence of new sharp features. Therefore, their detailed study was based on comparing the 2nd derivative spectra, which offered enhanced sensitivity, especially at low fixation temperatures where these bands are weak and overlapping with the strong and broad envelopes of H_2O modes (Figure 6).

In agreement with previous literature (Sposito *et al.*, 1983; Madejová *et al.*, 1996; Karakassides *et al.*, 1997; Gates, 2005; Madejová and Komadel, 2005), the envelope of Si−O stretching modes shifted to higher temperatures upon increasing fixation temperature. The trend was best monitored *via* the emergence of a sharp feature at 1123 cm^{-1} (similar to a pyrophyllite band at ~1120 cm^{-1}, Russell and Fraser, 1994) at the expense of a mode at ~1110 cm^{-1} (Figure 5) which corresponds to an in-plane Si−O stretching mode (Johnston and Premachandra, 2001).

In the range of OH-bending modes (Farmer, 1974), LiSAz-1_060 exhibited well defined bands at 911, 836, and 787 cm^{-1} which are commonly assigned to AlAlOH, AlMgOH, and possibly FeMgOH species, respectively (Madejová and Komadel, 2005; Gates, 2005). The assignment of the 787 cm^{-1} band may be questionable in the case of LiSAz-1 because of the low Fe content of this clay (Gates, 2005). Instead, this band should be attributed to silicate impurities. Montmorillonite exhibits a variable position of the main AlAlOH stretch fundamental in the range 3615−3630 cm^{-1} (Madejová *et al.* 1994; Bishop *et al.* 2002; Zviagina *et al.* 2004) whereas the first stretching overtone is found at ~7055−7090 cm^{-1} (Clark *et al.*, 1990; Bishop *et al.*, 2002), both overlapping with H_2O modes. Within these ranges, LiSAz-1_060 occupies an end-member position with low-energy positions of the AlAlOH fundamental and overtone modes at 3615 cm^{-1} and 7056 cm^{-1}, respectively (determined from the 2nd derivative spectra). High-wavenumber shoulders to these bands were observed at ~3650 cm^{-1}, as well as at 7125 and 7160 cm^{-1} (Figure 6). Whether these shoulders are due to AlMgOH species (*e.g.* Madejová *et al.* 1994) or to

https://doi.org/10.1346/CCMN.2013.0610207 Published online by Cambridge University Press

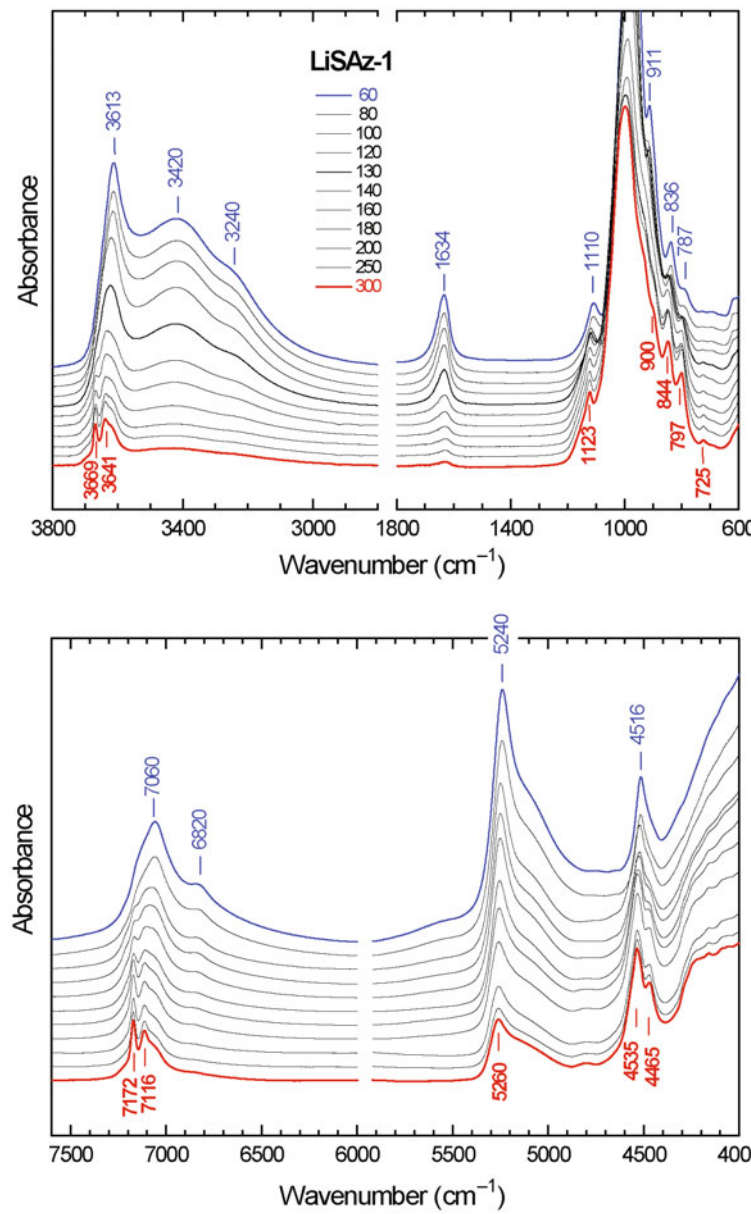

Figure 5. ATR (upper) and NIR (lower) absorption spectra of selected-reduced charge LiSAz-1 montmorillonites prepared by heating at various temperatures and fully equilibrated to ambient temperature. The spectra are offset for clarity and baseline corrected in the 6000−8000 cm^{-1} range.

pyrophyllite-type domains (Zviagina *et al.*, 2004) is not clear. Finally, the AlAlOH stretching-bending combination mode of dioctahedral aluminous smectites is typically observed in the 4520−4550 cm^{-1} range depending on composition (Post and Noble, 1993; Gates, 2005). LiSAz-1_060 exhibited this mode at 4518 cm^{-1} as a combination of the 911 and 3615 cm^{-1} fundamentals. A lower-wavenumber contribution at ~4445 cm^{-1} (Figure 6) is attributed to the corresponding AlMgOH combination mode (Gates, 2005).

Increasing Li fixation induces significant changes to the 2nd derivative spectra (Figure 6). A doublet of new OH-stretching fundamentals at 3641 and 3669 cm^{-1} (Δ = 28 cm^{-1}) grew progressively with increasing fixation temperature, accompanied by the corresponding overtones at 7116 and 7172 cm^{-1} (Δ = 56 cm^{-1}). In the range of the OH-bending fundamentals, new bands appeared at 797, 844, 896, and 927 cm^{-1}. Stretching-bending combinations were dominated by a sharp doublet at 4465 and 4538 cm^{-1} (Δ = 73 cm^{-1}), a higher-energy component below ~4570 cm^{-1}, and a number of low-wavenumber features below 4300 cm^{-1}. These spectral changes were resolved already upon heating at 100ºC and then evolved in parallel suggesting that their

https://doi.org/10.1346/CCMN.2013.0610207 Published online by Cambridge University Press

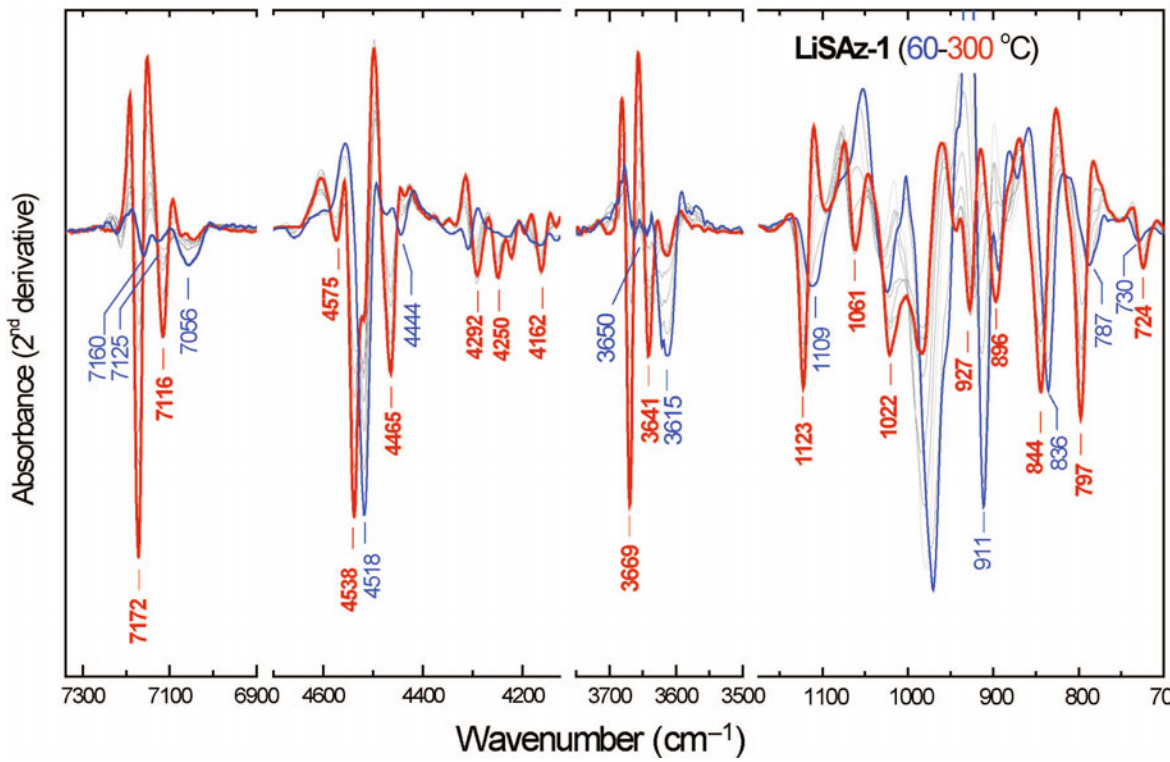

Figure 6. Second derivative absorption spectra of the RCM's based on LiSAz-1 over four ATR and NIR wavenumber ranges. The spectra corresponding to the lowest and highest fixation temperatures (60 and 300ºC) are shown using thick and thin lines (blue and red in the online version), respectively.

ensemble constituted the unique vibrational signature of Li fixation in SAz-1.

This description above of the spectral changes accompanying Li fixation is very similar to that reported by several authors on the basis of absorption spectra (Calvet and Prost, 1971; Madejová *et al.*, 2000a, 2000b; Petit *et al.*, 2004), with one subtle but important difference. These authors described the evolution in the OH-stretching (or overtone) range as the convolution of two processes: the progressive shift of the main ν_{01} (ν_{02}) OH mode of unheated montmorillonite towards 3641 cm^{-1} (7116 cm^{-1}) and the emergence of a new peak at 3669 cm^{-1} (7172 cm^{-1}). On the contrary, the 2nd derivative analysis demonstrates that the 3641 and 3669 cm^{-1} bands and their overtones at 7116 and 7172 cm^{-1} constitute pairs of fixed relative intensity which grow simultaneously at the expense of the broader 3615 (7056) cm^{-1} modes of unheated SAz-1. Moreover, the position and relative intensity of the component bands of the pair in the LiFEO-G system were identical to that of LiSAz-1, despite the large difference in octahedral layer charge of the two clay minerals (Figure 7). Stretching fundamental and overtone-OH modes at nearly identical positions were reported by Petit *et al*. (2002) for charge-reduced Fe-rich montmorillonite from Ölberg, Germany. Furthermore, the published IR absorption spectra of several reduced-charge montmorillonites with different octahedral charges suggest a very similar phenomenology. Prior to any heat treatment, the positions of their OH-stretching and overtone bands were quite variable, but when Li fixation was complete these converged to ~3640, 3670 cm^{-1} or 7110, 7170 cm^{-1}, respectively (Hrobáriková *et al.* 2001; Madejová *et al.*, 2000a, 2000b; Madejová, 2005).

Clearly, a unique self-consistent set of assignments is needed to describe the common vibrational signature of the Li-induced octahedral charge-reduction mechanism in montmorillonite.

Local structure of RCMs

A good starting point in deciphering the structure of RCMs is the assignment of the two ν_{01} bands at ~3640 and 3670 cm^{-1} and their ν_{02} counterparts at ~7115, 7170 cm^{-1}. These bands are attributed to structural OH species of the reduced-charge clay. However, their characteristic wavenumbers are intermediate to those typically encountered in dioctahedral and trioctahedral smectites (Farmer, 1974; Clark *et al.* 1990; Russell and Fraser, 1994) and could be assigned to either type of octahedral sheet. Even in the simplest case of neutral aluminous dioctahedral 2:1 clay minerals, the position of the AlAlOH stretching fundamental mode is highly variable. For example, in hydrated palygorskite, this

https://doi.org/10.1346/CCMN.2013.0610207 Published online by Cambridge University Press

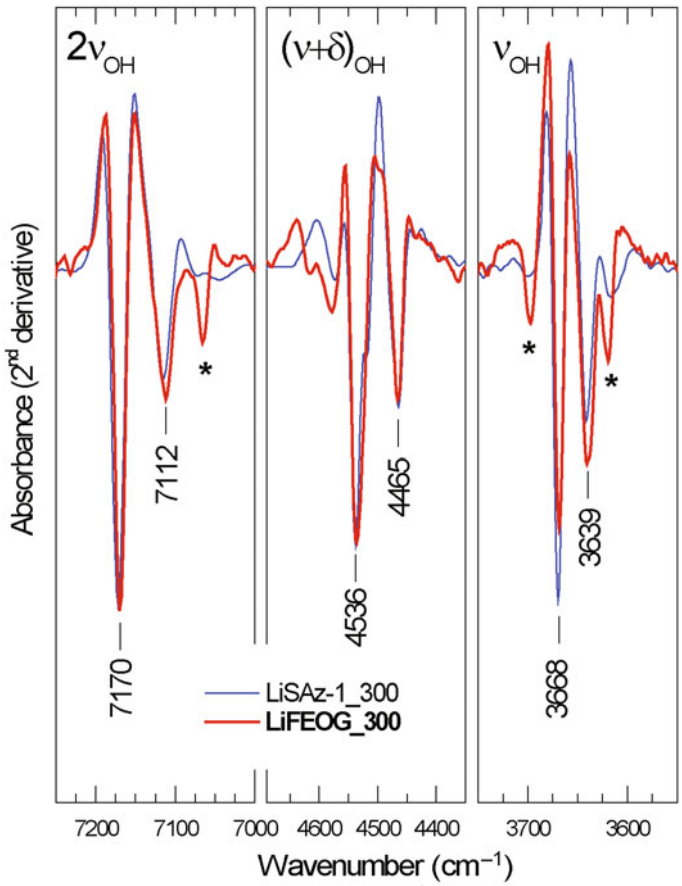

Figure 7. Comparison of the OH-stretching combination and overtone 2nd derivative spectra of LiFEO-G (thick line, red in online version) and LiSAz-1 (thin line, blue in online version) subjected to Li fixation at 300ºC. The spectrum of LiFEO-G is shown multiplied by a factor of 5. Peak positions correspond to LiFEO-G. Bands marked with asterisks are from a kaolinite ancillary phase.

mode is observed at 3615 cm^{-1}, shifting to 3624 cm^{-1} upon drying and to ~3645 cm^{-1} upon folding (VanScoyoc *et al.*, 1979; Gionis *et al.*, 2006). In pyrophyllite, it is observed at ~3675 cm^{-1}, *i.e.* in a position nearly identical to the Mg_3OH mode of talc (Russell and Fraser, 1994).

Insight into the nature of the new OH species can also be based on the anharmonicity values, $X = (2\nu_{01}-\nu_{02})/2$, which can be obtained with high precision from the 2nd derivative spectra. Thus, the data in Figure 6 indicate that both fundamental modes at ~3640 and 3670 cm^{-1} exhibit identical anharmonicity, $X = 83-84$ cm^{-1}, which is smaller than the value of $X = 87$ cm^{-1} of untreated montmorillonite SAz-1. The AlAlOH stretching of pyrophyllite with $\nu_{01} = 3675$ cm^{-1} and $\nu_{02} = 7177$ cm^{-1} (Russell and Fraser, 1994; Clark *et al.*, 1990; Kloprogge *et al.* 2000; Wang *et al.*, 2002) also yields $X = 87$ cm^{-1}. Values of anharmonicity in the range 87–88 cm^{-1} have also been reported for the AlAlOH, AlFeOH, and FeFeOH modes of (dioctahedral) palygorskite in both hydrated and dry states (Gionis *et al.*, 2006). These data indicate that the OH-stretching modes of dioctahedral 2:1 clay minerals exhibit rather uniform values of X, despite the aforementioned large energy variation of their fundamentals. In comparison, neutral trioctahedral 2:1 minerals such as talc or sepiolite have Mg_3OH stretching modes with lower anharmonicity values, $X = 84-85$ cm^{-1} (Petit *et al.*, 2004; Gionis *et al.*, 2007), closer to those observed in reduced-charge Li-montmorillonite. Based on the analysis above, the position of the OH-stretching modes alone is not useful in determining the exact nature of the absorbing species in RCMs, whereas the corresponding anharmonicity values point towards trioctahedral arrangements. The latter is in accordance with early reports for the pleochroism of these modes, which suggested that the OH bonds are perpendicular to the *ab* plane, as in trioctahedral minerals (Calvet and Prost, 1971). Then, the main question in interpreting the spectra is about a mechanism of charge reduction which could create simultaneously two OH-stretching modes (and their corresponding overtones) with fixed position and relative intensities.

That each type of OH species present yields a single OH-stretching (bending, *etc.*) vibrational mode is commonly accepted. Conversely, the number and

https://doi.org/10.1346/CCMN.2013.0610207 Published online by Cambridge University Press

relative intensity of OH bands are used to identify the various types of OH present in smectites and estimate their relative abundance (Farmer 1974; Madejová *et al.*, 1994; Besson and Drits, 1997a, 1997b; Gates *et al.*, 2002; Zviagina *et al.*, 2004; Petit, 2005; Gates, 2005; Gionis *et al.*, 2007; Chryssikos *et al.*, 2009). Assuming that this rule of thumb applies also in the case of RCMs, two possible explanations for the emergence of two ν_{01} OH-stretching modes (and their ν_{02} counterparts) can be proposed. Either fixed Li^+ modifies two pre-existing (but poorly distinguishable) populations of OH species and produces an equal number of sharp bands, or Li^+ interacts with a single type of OH group in a manner that removes their degeneracy and produces two new distinct populations.

The first scenario is usually linked to the presence of octahedral substitution by homovalent cations, *e.g.* Fe^{3+} for Al^{3+} in dioctahedral phyllosilicates. For example, the 3641 cm^{-1} peak (Figures 5–6) could represent the AlFeOH counterpart of an AlAlOH pyrophyllite-type mode at 3669 cm^{-1} (*cf.* Russell and Fraser, 1994; Besson and Drits, 1997b; Lantenois *et al.*, 2007). Alternatively, the two bands could correspond to AlMgLiOH and FeMgLiOH species. In either case, the relative intensity of the 3641 *vs.* 3669 cm^{-1} peaks should scale with $x/(1-x)$, where x is the fraction of Fe^{3+} in the octahedral sites. Obviously, this scaling is not supported by the fact that these peaks are identified in both low-Fe (SAz-1, FEO-G, this study) and high-Fe montmorillonites (Petit *et al.*, 2002).

The second scenario should involve the perturbation of AlMgOH in montmorillonite by Li^+. Two possibilities should be considered depending on whether the octahedral sheet is *cis*- or *trans*-vacant (*cv*, *tv*). In both cases, each Mg^{2+} cation substituting for Al^{3+} creates two crystallographically identical and energetically degenerate AlMgOH groups. Clearly, mechanisms of fixation capable of removing this degeneracy are required. One possibility would be to fit Li^+ inside a di-trigonal cavity of the tetrahedral sheet as suggested by some (Tettenhorst, 1962; Luca *et al.*, 1989; Alvero *et al.*, 1994; Theng *et al.*, 1997). In this manner, Li^+ would modify only one of the two AlMgOH groups. This type of mechanism would involve the coulombic interaction of Li^+ with the oxygen atom of the AlMgOH group and would lock the O-H dipole to a more tilted position with respect to the principal symmetry axis of the di-trigonal cavity. As such, this scenario is incompatible with the experimental finding that the OH groups of RCMs are perpendicular to the plane of the di-trigonal cavity (Calvet and Prost, 1971).

An alternative mechanism, which has been widely proposed to account for the spectra of RCMs and can remove the degeneracy of the OH groups, is the fixation of Li^+ inside octahedral vacancies (Figure 8). The presence of Li^+ would create local bonding rearrangements which would depend critically on the type of vacancy present. In the case of *cv* montmorillonite, one Li^+ cation occupying the M2a vacancy creates two equivalent AlMgLiOH groups (Figure 8, left), whereas the occupation of the M2b vacancy results in the formation of equivalent AlAlLiOH groups (not shown). In contrast, charge reduction involving the occupation of the M1a *trans*-vacancies by Li^+ is the only mechanism enabling the degeneracy removal of the pre-existing AlMgOH and AlAlOH units by creating AlMgLiOH and AlAlLiOH species in a 1:1 ratio (Figure 8, right). Clearly, this last scenario is compatible with the synchronous appearance of two sharp trioctahedral-like OH stretching (and overtone) modes with fixed position and relative intensity upon charge reduction. If the above argument is correct, the unique vibrational signature of RCMs (Figure 7) would be linked to the presence of *tv* domains in both montmorillonites, and these are more abundant in SAz-1 than in LiFEO-G.

According to Tsipurski and Drits (1984), montmorillonite can range from 100% *cv* (represented by a Wyoming low charge montmorillonite) to 100% *tv*, whereas illite, beidellite, and nontronite are considered to be primarily *trans*-vacant. However, a clear correlation between the composition or the charge of montmorillonite and the type of octahedral vacancy has not been established experimentally (Drits and Zviagina, 2009). The previous published IR studies have not suggested a distinction between the two types of octahedral domains in montmorillonite. As a result, the only practical estimation of the prevailing type of vacancy is based on the proposal by Drits *et al.* (1995), who related the type of vacancy in aluminous dioctahedral smectites indirectly to their temperature of dehydroxylation: *cv* smectites dehydroxylate at temperatures ~150–200ºC higher than their *tv* counterparts (*cf.* Wolters and Emmerich, 2007). A dehydration threshold between the two types (~600ºC) is commonly accepted, according to which SAz-1 and FEO-G (~635ºC) are on the low-end of the *cv* range. Theoretical modeling of *cv* and *tv* illites and smectites (Sainz-Diaz *at al.*, 2001) have suggested that *tv* configurations are slightly favored over their *cv* analogs upon increasing octahedral Mg content and layer charge. These studies would classify SAz-1 and FEO-G as *tv* smectites.

Clearly, the systematics of the octahedral vacancies in montmorillonite remain poorly understood. The present analysis suggests that Li^+ fixation followed by 2^{nd} derivative mid- or near-IR spectroscopy may enhance the 'structural contrast' between *cis*- and *trans*-vacancies, and therefore become a convenient tool for estimating their relative abundance.

CONCLUSIONS

The gradual reduction of the layer charge of two montmorillonites with different layer charge, due to the Hoffmann-Klemen effect, was studied by Li saturation

https://doi.org/10.1346/CCMN.2013.0610207 Published online by Cambridge University Press

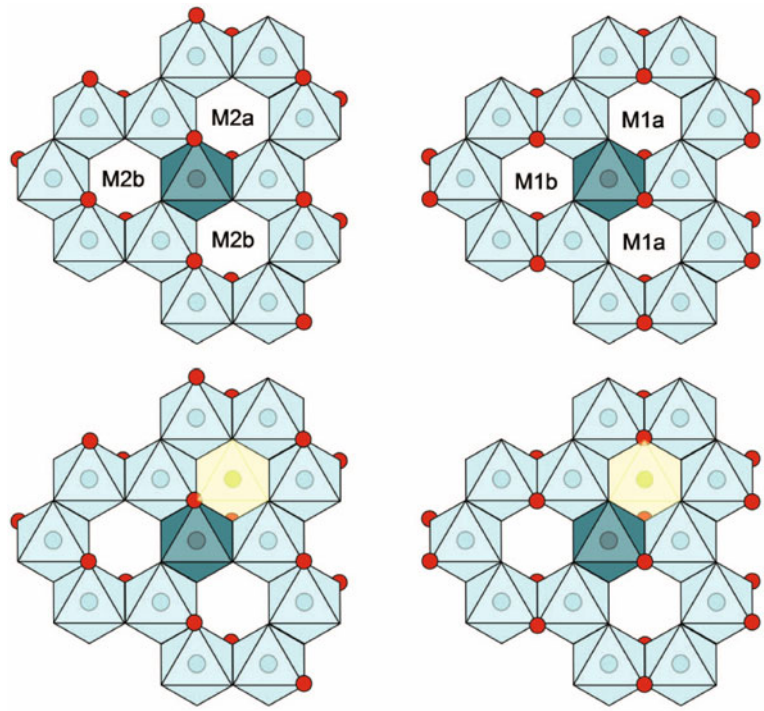

Figure 8. Schematic structure of the octahedral sheet in *cv* (upper left) and *tv* (upper right) montmorillonite with the structural OH groups shown as small spheres. Both arrangements result in two degenerate AlMgOH groups per octahedral Mg^{2+}. The AlAlOH groups are also degenerate in both cases. The degeneracy is preserved by Li^{+} fixation in either the M2a (lower left) or the M2b *cis* vacancy. The degeneracy of the two types of OH groups is removed only if Li^{+} occupies an M1a *trans*-octahedral vacancy (lower right), creating AlMgLiOH, AlAlLiOH units in addition to unperturbed AlMgOH and AlAlOH.

and heating at 80−300ºC. The migration of Li in vacant octahedral sites was accompanied by a decrease in layer charge, CEC, and the amount of adsorbed water, whereas the dehydroxylation temperature remained unaffected. In both smectites, a residual CEC was observed at the end of the experiments, which is attributed to residual vacant octahedral sites due to kinetic constraints. Upon Li migration to vacant octahedral sites, two new sharp OH-stretching fundamentals at ~3640 and 3670 cm^{-1} and their overtones at ~7115, 7170 cm^{-1} were observed in the FTIR spectra of both smectites. Various models of Li fixation capable of removing the degeneracy of the original AlMgOH species were examined. On this basis, the changes observed in the FTIR spectra after Li fixation were compatible with Li^{+} occupying *trans* octahedral vacancies in both smectites. The results of the present study will shed light on the *cis/trans* configuration of smectites and on their behavior at the low charge limit (0.2 e/huc).

ACKNOWLEDGMENTS

This work was funded by a Basic Research Grant to GEC by the Technical University of Crete, as well as by the Applied Spectroscopy Laboratory of TPCI/NHRF. The constructive comments of the Associate Editor and two anonymous reviewers improved the text.

REFERENCES

Alba, M.D., Alvero, R., Becerro, A.I., Castro, M.A., and Trillo, J.M. (1998) Chemical behaviour of lithium ions in reexpanded Li-montmorillonites. *Journal of Physical Chemistry B*, **102**, 2207−2213.

Alvero, R., Alba, M.D., Castro, M.A., and Trillo, J.M. (1994) Reversible migration of lithium in montmorillonite. *Journal of Physical Chemistry*, **98**, 7848−7853.

Bain, D.C. and Smith, B.F.L. (1987) Chemical analysis. Pp. 248−274 in: *A Handbook of Determinative Methods in Clay Mineralogy* (M.J. Wilson, editor). Blackie, Glasgow and London.

Besson, G. and Drits, V.A. (1997a) Refined relationships between chemical composition of dioctahedral fine-dispersed mica minerals and their infrared spectra in the OH stretching region. Part I: Identification of the stretching bands. *Clays and Clay Minerals*, **45**, 158−169.

Besson, G. and Drits, V.A. (1997b) Refined relationships between chemical composition of dioctahedral fine-dispersed mica minerals and their infrared spectra in the OH stretching region. Part II: The main factors affecting OH vibration and quantitative analysis. *Clays and Clay Minerals*, **45**, 170−183.

Bishop, J., Pieters, C.M., and Edwards, J.O. (1994) Infrared spectroscopic analyses on the nature of water in montmorillonite. *Clays and Clay Minerals*, **42**, 702−716.

Bishop, J., Madejová, J., Komadel, P., and Fröschl, H. (2002) The influence of structural Fe, Al and Mg on the infrared OH bands in spectra of dioctahedral smectites. *Clay Minerals*, **37**, 607−616.

Brigatti, M.F., Galán, E., and Theng, B.K.G. (2006) Structures and mineralogy of clay minerals. Pp. 19−86 in: *Handbook of Clay*

https://doi.org/10.1346/CCMN.2013.0610207 Published online by Cambridge University Press

Science (F. Bergaya, G. Lagaly and B.K.G. Theng, editors). Developments in Clay Science, **1**, Elsevier, Amsterdam.

Brindley, G.W. and Ertem, G. (1971) Preparation and solvation properties of some variable charge montmorillonites. *Clays and Clay Minerals*, **19**, 399–404.

Bujdák, J., Janek, M., Madejová, J., and Komadel, P. (2001) Methylene blue interactions with reduced charge smectites. *Clays and Clay Minerals*, **49**, 244–254.

Calvet, R. and Prost, R. (1971) Cation migration into empty octahedral sites and surface properties of clays. *Clays and Clay Minerals*, **19**, 175–186.

Christidis, G.E. (2006) Genesis and compositional heterogeneity of smectites. Part III: Alteration of basic pyroclastic rocks – A case study from the Troodos Ophiolite Complex, Cyprus. *American Mineralogist*, **91**, 685–701.

Christidis, G.E. and Eberl, D.D. (2003) Determination of layer charge characteristics of smectites. *Clays and Clay Minerals*, **51**, 644–655.

Christidis, G.E., Blum, A.E., and Eberl, D.D. (2006) Influence of layer charge and charge distribution of smectites on the flow behaviour and swelling of bentonites. *Applied Clay Science*, **34**, 125–138.

Chryssikos, G.D., Gionis, V., Kacandes, G.H., Stathopoulou, E.T., Suárez, M., García-Romero, E., and Sánchez del Río, M. (2009) Octahedral cation distribution in palygorskite. *American Mineralogist*, **94**, 200–203.

Clark, R.N., King, T.V.V., Klejwa, M., Swayze, G.A., and Vergo, N. (1990) High spectral resolution reflectance spectroscopy of minerals. *Journal of Geophysical Research*, **95**, 12653–12680.

Drits, V.A. and Zviagina, B.B. (2009) *Trans*-vacant and *cis*-vacant 2:1 layer silicates: Structural features, identification, and occurrence. *Clays and Clay Minerals*, **57**, 405–415.

Drits, V.A., Besson, G., and Muller, F. (1995) An improved model for structural transformations of heat-treated aluminous dioctahedral 2:1 layer silicates. *Clays and Clay Minerals*, **43**, 718–731.

Farmer, V.C. (1974) The layer silicates. Pp. 331–363 in: *The Infrared Spectra of Minerals* (V.C. Farmer, editor). Monograph **4**, Mineralogical Society, London.

Gates, W.P. (2005) Infrared spectroscopy and the chemistry of dioctahedral smectites. Pp. 125–168 in: *The Application of Vibrational Spectroscopy to Clay Minerals and Layered Double Hydroxides* (J.T. Kloprogge, editor). CMS Workshop Lectures **13**, The Clay Minerals Society, Aurora, Colorado, USA.

Gates, W.P., Komadel, P., Madejová, J., Bujdák, J., Stucki, J.W., and Kirkpatrick, R.J. (2000) Electronic and structural properties of reduced-charge montmorillonites. *Applied Clay Science*, **16**, 257–271.

Gates, W.P., Slade, P.G., Manceau, A., and Lanson, B. (2002) Site occupancies by iron in nontronites, *Clays and Clay Minerals*, **50**, 223–239.

Gionis, V., Kacandes, G.H., Kastritis, I.D., and Chryssikos, G.D. (2006) On the structure of palygorskite by mid- and near-infrared spectroscopy. *American Mineralogist*, **91**, 1125–1133.

Gionis, V., Kacandes, G.H., Kastritis, I.D., and Chryssikos, G.D. (2007) Combined near-infrared and X-ray diffraction investigation of the octahedral sheet composition of palygorskite. *Clays and Clay Minerals*, **55**, 543–553.

Guggenheim, S. and Koster van Groos, A.F. (2001) Baseline studies of the Clay Minerals Society Source clays: Thermal Analysis. *Clays and Clay Minerals* **49**, 433–443.

Guisseau, D., Patrier Mas, P., Beaufort, D., Girard, J.-P., Inoue, A., Sanjuan, B., Petit, S., Arnaud Lens, A., and Genter, A. (2007) Significance of the depth-related transition montmorillonite-beidellite in the Bouillante geothermal field (Guadeloupe, Lesser Antilles). *American Mineralogist*, **92**, 1800–1813

Greene-Kelly, R. (1953) The identification of montmorillonoids in clays. *Journal of Soil Science*, **4**, 233–237.

Güven, N. (1992) Rheological aspects of aqueous smectite suspensions. Pp. 81–125 in: *Clay–Water Interface and its Rheological Implications* (N. Güven and R.M. Pollastro, editors). CMS Workshop Lectures **4**, The Clay Minerals Society, Bloomington, Indiana, USA.

Hofmann, U. and Klemen, R. (1950) Verlust der Austauschfahigkeit von Lithiumionen an Bentonit durch Erhitzung. *Zeitschrift für Anorganische und Allgemeine Chemie*, **262**, 95–99.

Hrobáriková, J., Madejová, J., and Komadel, P. (2001) Effect of heating temperature on Li fixation, layer charge and properties of fine fractions of bentonites. *Journal of Materials Chemistry*, **11**, 1452–1457.

Jaynes, W.F. and Bigham, J.M. (1987) Charge reduction, octahedral charge, and lithium retention in heated, Li-saturated smectites. *Clays and Clay Minerals*, **35**, 440–448.

Johnston, C.T. and Premachandra, G.S. (2001) Polarized ATR-FTIR study of smectite in aqueous suspension. *Langmuir*, **17**, 3712–3718.

Karakassides, M.A., Petridis D., and Gournis, D. (1997) Infrared Reflectance Study of Thermally Treated Li- and Cs-Montmorillonites. *Clays and Clay Minerals*, **45**, 649–658.

Karakassides, M.A., Madejová, J., Arvaiová, B., Bourlinos, A., Petridis, D., and Komadel, P. (1999) Location of Li(I), Cu(II), and Cd(II) in heated montmorillonite: Evidence from specular reflectance infrared and electron spin resonance spectroscopies. *Journal of Materials Chemistry*, **9**, 1553–1558.

Kloprogge, J.T., Ruan, H., and Frost, R.L. (2000) Near-infrared spectroscopic study of synthetic and natural pyrophyllite. *Neues Jahrbuch für Mineralogie, Monatshefte*, **2000**, 337–347.

Komadel, P. (2003) Chemically modified smectites. *Clay Minerals*, **38**, 127–138.

Komadel, P., Bujdák, J., Madejová, J., Šucha, V., and Elsass, F. (1996) Effect of non-swelling layers on the dissolution of reduced-charge montmorillonite in hydrochloric acid. *Clay Minerals*, **31**, 333–345.

Koster van Groos, A.F. and Guggenheim, S. (1987) Dehydration of a Ca-and a Mg-exchanged montmorillonite (SWy-1) at elevated pressures. *American Mineralogist*, **72**, 292–298.

Laird, D.A. (1999) Layer charge influences on the hydration of expandable 2:1 phyllosilicates. *Clays and Clay Minerals*, **47**, 630–636.

Laird, D.A. (2006) Influence of layer charge on swelling of smectites. *Applied Clay Science*, **34**, 74–87.

Laird, D.A. and Fleming, P. (2008) Analysis of layer charge, cation and anion exchange capacities, and synthesis of reduced charge clays. In: *Methods of Soil Analysis. Part 5. Mineralogical Methods* (A. Ulery and R. Drees, editors). SSSA Book Series No 5. Madison, Wisconsin.

Laird, D.A., Barriuso, E., Dowdy, R.H., and Koskinen, W.C. (1992) Adsorption of atrazine on smectites. *Soil Science Society of America Journal*, **56**, 62–67.

Lantenois, S., Beny, J.-M., Muller, F., and Champallier, R. (2007) Integration of Fe in natural and synthetic Al-pyrophyllites: an infrared spectroscopic study. *Clay Minerals*, **42**, 129–141.

Lim, C.H. and Jackson, M.L. (1986) Expandable phyllosilicate reactions with lithium on heating. *Clays and Clay Minerals*, **34**, 346–352.

Luca, V., Cardile, C.M., and Meinhold, R.H. (1989) High resolution multinuclear NMR study of cation migration in montmorillonite. *Clay Minerals*, **24**, 115–119.

Madejová, J. (2005) Studies of reduced-charge smectites by near infrared spectroscopy. Pp. 169–202 in: *The Application*

of Vibrational Spectroscopy to Clay Minerals and Layered Double Hydroxides (J.T. Kloprogge, editor). CMS Workshop Lectures **13**, The Clay Minerals Society, Aurora, Colorado, USA.

Madejová, J. and Komadel, P. (2005) Information available from infrared spectra of the fine fractions of bentonites. Pp. 65–98 in: *The Application of Vibrational Spectroscopy to Clay Minerals and Layered Double Hydroxides* (J.T. Kloprogge, editor). CMS Workshop Lectures **13**, The Clay Minerals Society, Aurora, Colorado, USA.

Madejová, J., Komadel, P., and Čičel, B. (1994) Infrared study of octahedral site populations in smectites. *Clay Minerals*, **29**, 319–326.

Madejová, J., Bujdák, J., Gates, W.P., and Komadel, P. (1996) Preparation and infrared spectroscopic characterization of reduced-charge montmorillonite with various Li contents. *Clay Minerals*, **31**, 233–241.

Madejová, J., Bujdák, J., Petit, S., and Komadel, P. (2000a) Effects of chemical composition and temperature of heating on the infrared spectra of Li-saturated dioctahedral smectites (I) Mid-infrared region. *Clay Minerals*, **35**, 739–751.

Madejová, J., Bujdák, J., Petit, S., and Komadel, P. (2000b) Effects of chemical composition and temperature of heating on the infrared spectra of Li-saturated dioctahedral smectites (II) Near-infrared region. *Clay Minerals*, **35**, 753–761.

Madejová, J., Pálková, H., and Komadel, P. (2006) Behaviour of Li^{+} and Cu^{2+} in heated montmorillonite: Evidence from far-, mid-, and near-IR regions. *Vibrational Spectroscopy*, **40**, 80–88.

Maes, A. and Cremers, A. (1977) Charge density effects in ion exchange. Part 1. Heterovalent exchange equilibria. *Journal of the Chemical Society Faraday Transactions*, **73**, 1807–1814.

Maes, A. and Cremers, A. (1978) Charge density effects in ion exchange. Part 2. Homovalent exchange equilibria. *Journal of the Chemical Society Faraday Transactions*, **74**, 1234–1241.

Maes, A., Stul, M.S., and Cremers, A. (1979) Layer charge-cation-exchange capacity relationships in montmorillonite. *Clay and Clay Minerals*, **27**, 387–392.

Muller, F., Besson, G., Manceau, A., and Drits, V.A. (1997) Distribution of isomorphous cations within octahedral sheets in montmorillonite from Camp-Berteau. *Physics and Chemistry of Minerals*, **24**, 159–166.

Odom, I.E. (1984) Smectite clay minerals: properties and uses. *Philosophical Transactions of the Royal Society of London*, **A311**, 391–409.

Petit, S. (2005) Crystal-chemistry of talcs: A NIR and MIR spectroscopic approach. Pp. 41–64 in: *The Application of Vibrational Spectroscopy to Clay Minerals and Layered Double Hydroxides* (J.T. Kloprogge, editor). CMS Workshop Lectures **13**, The Clay Minerals Society, Aurora, Colorado, USA.

Petit, S., Caillaud, J., Righi, D., Madejová, J., Elsass, F., and Köster, H.M. (2002) Characterization and crystal chemistry of an Fe-rich montmorillonite from Ölberg, Germany. *Clay Minerals*, **37**, 283–297.

Petit, S., Decarreau, A., Martin, F., and Buchet, R. (2004) Refined relationship between the position of the fundamental OH stretching and the first overtones for clays. *Physics and Chemistry of minerals*, **31**, 585–592.

Post J.L. and Noble, P.N. (1993) The near-infrared combination band frequencies of dioctahedral smectites, micas and illites. *Clays and Clay Minerals*, **41**, 639–644.

Russell, J.D. (1979) An infrared spectroscopic study of the interaction of nontronite and ferruginous montmorillonites with alkali metal hydroxides. *Clay Minerals*, **14**, 127–137.

Russell, J.D. and Fraser, A.R. (1994) Infrared methods. Pp. 11–67 in: *Clay Mineralogy: Spectroscopic and Chemical Determinative Methods* (M.J. Wilson, editor). Chapman & Hall, London.

Sainz-Diaz, C.I., Hernández-Laguna, A., and Dove, M.T. (2001) Theoretical modelling of *cis*-vacant and *trans*-vacant configurations in the octahedral sheet of illites and smectites. *Physics and Chemistry of Minerals*, **28**, 322–331.

Sato, T., Watanabe, T., and Otsuka, R. (1992) Effects of layer charge, charge location and energy change on expansion properties of dioctahedral smectites. *Clays and Clay Minerals*, **40**, 103–113.

Shainberg, I., Alperovitch, N.I., and Keren, R. (1987) Charge density and Na–K–Ca exchange on smectites. *Clays and Clay Minerals*, **35**, 68–73.

Slade, P.G., Quirk, J.R., and Norrish, K. (1991) Crystalline swelling of smectite samples in concentrated NaCl solutions in relation to layer charge. *Clays and Clay Minerals*, **39**, 234–238.

Sposito, G., Prost, R., and Gaultier, J.P. (1983) Infrared spectroscopic study of adsorbed water on reduced-charge Na/Li-montmorillonites. *Clays and Clay Minerals*, **31**, 9–16.

Srasra, E., Bergaya, F., and Fripiat, J.J. (1994) Infrared spectroscopy study of tetrahedral and octahedral substitutions in an interstratified illite-smectite clay. *Clays and Clay Minerals*, **42**, 237–241.

Stackhouse, S. and Coveney, P.V. (2002) Study of thermally treated lithium montmorillonite by *ab initio* methods. *Journal of Physical Chemistry*, **106**, 12470–12477.

Tettenhorst, R. (1962) Cation migration in montmorillonites. *American Mineralogist*, **47**, 769–773.

Theng, B.K.G., Hayashi, S., Soma, M., and Seyama, H. (1997) Nuclear magnetic resonance and X-ray photoelectron spectroscopic investigation of lithium migration in montmorillonite. *Clays and Clay Minerals*, **45**, 718–723.

Tombacz, E. and Szekeres, M. (2004) Colloidal behaviour of aqueous montmorillonite suspensions: the specific role of pH in the presence of indifferent electrolytes. *Applied Clay Science*, **27**, 75–94.

Tsipurski, S.I. and Drits, V.A. (1984) The distribution of octahedral cations in the 2:1 layers of dioctahedral smectites studied by oblique-texture electron diffraction. *Clay Minerals*, **19**, 177–193.

VanScoyoc, G.E., Serna, C.J., and Ahlrichs, J.L. (1979) Structural changes in palygorskite during dehydration and dehydroxylation. *American Mineralogist*, **64**, 215–223.

Wolters, F. and Emmerich, K. (2007) Thermal reactions of smectites – Relation of dehydroxylation temperature to octahedral structure. *Thermochimica Acta*, **462**, 80–88.

Wang, L., Zhang, M., Redfern, S.A.T., and Zhang, Z. (2002) Dehydroxylation and transformations of the 2:1 phyllosilicate pyrophyllite at elevated temperatures: An infrared spectroscopic study. *Clays and Clay Minerals*, **50**, 272–283.

Zviagina, B.B., McCarty, D.K., Środoń, J., and Drits, V.A. (2004) Interpretation of infrared spectra of dioctahedral smectites in the region of OH-stretching vibrations. *Clays and Clay Minerals*, **52**, 399–410.

(*Received 13 August 2012; revised 23 February 2013; Ms. 700, AE: S. Petit*)